ChemComm

COMMUNICATION

View Article Online
View Journal | View Issue

Cite this: *Chem. Commun.*, 2024, **60**, 7160

Received 29th May 2024,
Accepted 17th June 2024

DOI: 10.1039/d4cc02603a

rsc.li/chemcomm

Length dependent reversible off–on activation of photo-switchable relay anion transporters†

Toby G. Johnson, Amir Sadeghi-Kelishadi and Matthew J. Langton *

A homologous series of azobenzene-derived photo-switchable ion relay transporters is reported. We reveal that both the length and geometry of the relay strongly affect transport rate, allowing the relative activity of the *E* and *Z* isomers to be reversed and hence the wavelengths of light used for on and off switching to be exchanged.

Ion transport processes in nature are regulated by sophisticated protein channels which themselves respond to external stimuli including ligand binding, membrane potential and light.[1] To gain a better understanding of ion transport processes across lipid bilayers, numerous synthetic ion transport systems have been developed.[2–5] Such systems may also hold potential as future therapeutics.[6,7] Stimuli-responsive activity has been engineered into synthetic transporters, mimicking biological transport systems.[8–10] Synthetic transporters operating *via* a mobile carrier mechanism have been reported which respond to redox,[11,12] pH,[13,14] membrane potential,[15] enzymes[16,17] and light.[17–26] Generally, a blocking group is appended to the receptor unit of the transporter which is cleaved in response to stimulation, irreversibly turning on transport.[22,24,25] Reversible switching of mobile carrier activity is rarer, however examples of redox[11] as well as light responsive systems have been reported which display temporal control of transport activity within the lipid membrane environment.[18,20,23]

Anchored carriers represent an emerging class of transporters which operate *via* an abiotic mechanism.[27,28] The first example of an anchored carrier was reported by Smith *et al.* in 2008, where a lipid-anchored urea-based transporter facilitated anion transport *via* a relay mechanism.[29] We have since demonstrated that halogen bonding iodotriazole-based relay transporters significantly improve transport activity, as well as displaying high $Cl^- > OH^-$ ion transport selectivity.[30] Through the incorporation of a tetra-*ortho*-fluoroazobenzene photoswitch within the relay, we have also developed a photo-responsive system in which *in situ*, visible light mediated photo-isomerisation enabled reversible control of transport activity.[31] The isomeric state of the photoswitch served to control the length of the telescopic carrier arm, whereby transport activity was observed to be greater for the longer *E*-isomer compared to the shorter *Z*-isomer.

The control of relay transporters relies on precise geometric control of the receptors in opposite leaflets of the bilayer. However, there is little understanding as to what molecular features lead to efficient relay transport, or effective photo-switching of activity. Herein, we explore the visible light regulated anion transport capability of a homologous series of photo-switchable relay transporters **1–3** of varying carrier arm length (Fig. 1). We show that the dramatic changes in transport activity with increasing relay length can be exploited to completely reverse the switching sense of the relay, such that the *Z*-isomer is more active that the *E*-isomer in the longer derivatives, and that off–on switching can be controlled using the opposite combination of wavelengths to the previously reported shorter relay transporters.[31]

Relay transport proceeds *via* the mechanism shown in Fig. 1A.[27] A membrane-anchored receptor in the outer leaflet

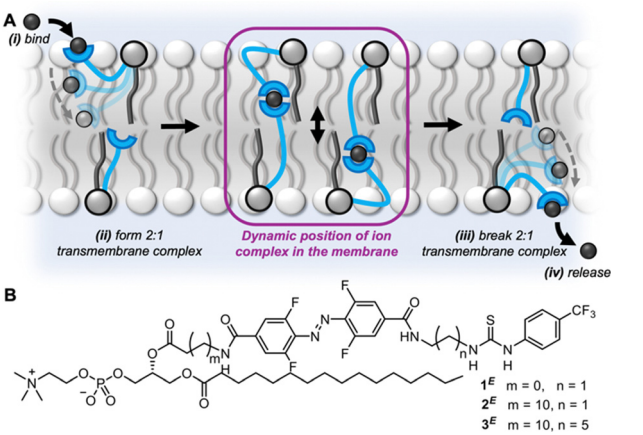

Fig. 1 (A) Schematic representation of the relay transport mechanism. (B) Photo-switchable relay transporters (**1–3**) of varying relay carrier arm length.

Chemistry Research Laboratory, Mansfield Road, Oxford, OX1 3TA, UK.
E-mail: matthew.langton@chem.ox.ac.uk

† Electronic supplementary information (ESI) available. See DOI: https://doi.org/10.1039/d4cc02603a

binds to an ion at the outer water-membrane interface bringing it into the membrane. The ion is exchanged with a partner receptor, anchored in the opposite leaflet of the bilayer, which can release the ion to the inner aqueous environment. Relay transporters are unable to span the length of the bilayer to facilitate transport of the ion *via* a unimolecular "fishing" mechanism.[32–35] We sought to explore the effect of varying the length of the relay transporter on the photo-switching of transport activity in a homologous series **1–3** (Fig. 1B).

The photo-switchable relay transporters **1** and **2** were prepared as previously described,[31] from the corresponding amino-functionalised phospholipid *via* coupling to an activated ester of the azobenzene relay arm and subsequent thiourea formation. The novel extended relay transporter **3** was synthesised following a similar strategy (see ESI† for full synthetic details). The photophysical properties of **3** were first investigated in $CDCl_3$: CD_3OD (2 : 1) using ^{1}H NMR experiments following irradiation with an LED (405 nm or 530 nm) to generate the photo-stationary state (PSS) distribution (Fig. S16, ESI†). Efficient bidirectional switching was observed, with the PSS distributions for both the *E*-isomer rich (PSS_{405} *E* : *Z* 96 : 4) and *Z*-isomer rich (PSS_{530} *E* : *Z* 10 : 90) populations matching those previously reported for **1** and **2**.[31] The photostability of **3** after prolonged irradiation in solution was evaluated by ^{1}H NMR, which displayed no observable degradation after irradiation with 405 nm (1000 mW) or 530 nm (370 nm) light for up to 20 minutes (Fig. S17 and 18, ESI†). The UV-vis absorbance spectrum of **3** in DMSO following irradiation of the sample with light (405 nm or 530 nm) displayed a red-shift of the n → π* absorption band of $\mathbf{3}^{E}$ relative to $\mathbf{3}^{Z}$, characteristic of the tetra-*ortho*-fluoroazobenzene core which enables photo-switching with visible light (Fig. S20, ESI†).[36,37]

The transport activity of **3**, in comparison to the shorter derivatives **1** and **2**, was investigated in large unilamellar vesicles (LUVs) using fluorescence assays. The pH-sensitive fluorescent probe 8-hydroxypyrene-1,3,6-trisulfonic acid (HPTS) was encapsulated within 1-palmitoyl-2-oleoyl-*sn*-glycero-3-phosphocholine vesicles (POPC LUVs, 200 nm diameter), which were suspended in NaCl (100 mM) solution, buffered to pH 7.0 with HEPES (10 mM). A base pulse of NaOH (5 mM) was added to generate a pH gradient, while measuring the ratiometric fluorescence of HPTS (λ_{em} = 510 nm, λ_{ex} = 405/460 nm) allowed the internal pH of the LUVs to be monitored. Transport activity was first evaluated by external addition of the lipid anchored transporters to pre-formed POPC LUVs, such that the transporters are added solely to the outer leaflet. The change in internal pH of the vesicles was minimal when either isomer of the three transporters was added externally (Fig. 2A and B, dashed lines), demonstrating the requirement for relays to be present in both leaflets of the membrane, and revealing the inability of phospholipid anchored relays to translocate across the lipid bilayer from the outer leaflet to the inner leaflet. This data also reveals that the longer derivative is not of sufficient length to facilitate transport *via* a fishing mechanism,[32] in which an anchored carrier can individually mediate anion transport across the entire membrane, without requiring a receiving relay in the opposite leaflet.[27] This was also true in LUVs composed of lipids of varying acyl chain lengths (14 : 0‡, 16 : 1, 18 : 1 and 20 : 1 *cis*-phosphatidylcholine) - no activity was observed in these lipids following external relay addition (Fig. S23, ESI†).

Next, the activity of **3** in comparison to **1** and **2** was evaluated by pre-incorporation of the lipid anchored transporters in various concentrations in POPC LUVs during vesicle preparation, in order to generate an equal distribution of relay transporters in both leaflets of the membrane. The LUVs were pre-irradiated to establish the PSS within the bilayer[31] (405/530 nm, 2 min), before addition of the base pulse to start the assay. The thermal half-lives of these photoswitches is known to be in the order of months[36,37] and we have previously shown that in the bilayer environment the long thermal half-lives of the photoswitchable relay transporters are maintained, such that negligible

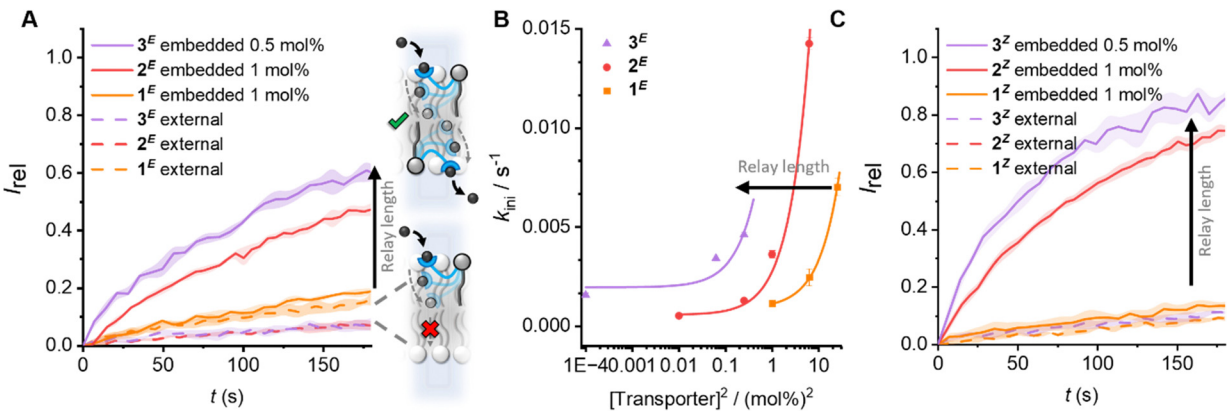

Fig. 2 The effect of carrier arm length on relay transport activity. (A) Anion transport data for *E*-isomers. Data shows change in ratiometric emission, I_{rel} (λ_{em} = 510 nm; λ_{ex1} = 405 nm, λ_{ex2} = 460 nm), upon addition of a NaOH base pulse (5 mM) to POPC LUVs (31 μM) containing 1 mM HPTS, 100 mM internal and external NaCl, buffered with 10 mM HEPES at pH 7.0. Concentrations given as mol% with respect to lipid. Data for relay transporters pre-incorporated during LUV preparation (solid lines, following *in situ* irradiation with 405 nm light to generate *E*-rich PSS) or added externally to pre-formed vesicles (dashed lines, in 5 μL DMSO following irradiation, 1 mol%). The shaded area represents the standard error of three runs. (B) Initial rates of transport for the *E*-isomers, and fit to a 2nd order rate equation. (C) Data for the corresponding *Z*-isomers (following irradiation with 530 nm light, conditions as in (A)). Data for **1** and **2** from ref. 31.

change in isomer distribution occurs over the course of the transport assay.[31] The anion transport activity of the *E*-rich PSS distributions of relays **1–3** are shown in Fig. 2A (solid lines). A dependence on the initial transport rate with the square of the transporter concentration for $\mathbf{3}^{E}$ reveals a bimolecular rate-limiting step, as previously observed with shorter relay derivatives[29–31] (Fig. 2B). This is consistent with the breaking of a membrane spanning relay transporter-ion complex in the rate-limiting step (Fig. 1(iii)). The same rate dependence observed across **1–3** suggests that the three extended derivatives all operate *via* the same relay mechanism. Analysis of the transport rates of **1–3** indicates that the observed transport activity increases with the length of the relay arm (Fig. 2). By preparing asymmetric membrane distributions of relay transporters, we have previously shown that dissociation of a transient 2 : 1 transmembrane complex is rate limiting,[30,31] presumably due to the low dielectric in the membrane interior enhancing binding anion affinity.[38,39] Across the homologous series of $\mathbf{1}^{E}$–$\mathbf{3}^{E}$, the anion binding thiourea is identical, and so all other factors being equal, the rates of binding, exchange and release steps should be identical. However, anion affinity is also a function of local dielectric.[40,41] We therefore suggest that the different lengths of the relay transporters vary the position within the bilayer at which the transient 2 : 1 transporter-ion complex dissociation occurs (Fig. 1A). For the shortest derivative $\mathbf{1}^{E}$, dissociation will occur closest to the centre of the bilayer where the dielectric constant is lowest, and the affinity of the receptor to the anion is highest. With increasing relay transporter carrier arm length, the increased transport activity suggests that dissociation becomes more favourable, likely resulting from the ability to break the transporter-ion complex further from the centre of the bilayer, in a region of the membrane in which the dielectric constant is higher and the complex is less stable.

We next compared the activity of the *Z*-isomers of the relay transporters of differing lengths by generating the corresponding *Z*-rich PSS by irradiation with 530 nm light. As with the *E*-isomers, external addition to the outer leaflet did not result in transport (Fig. 2C, dashed lines). When incorporated into both leaflets, the same trend of increasing activity with lengthening of the carrier arm was observed (Fig. 2C, solid lines). Analysis of the initial rates of transport also revealed a dependence on the square of the relay concentration (Fig. S25, ESI†), suggesting that, as with the *E*-isomers, the rate limiting step is dissociation of a membrane-spanning 2 : 1 relay-anion complex. As shown previously, for the shorter derivative **1**, the contracted *Z*-isomer displayed a reduction in transport activity relative to the extended *E*-configuration (Fig. 3A), due to the inability of the contracted relay to form the required transient membrane-spanning 2 : 1 relay-anion complex.[31] Interestingly, however, with the longer derivatives **2** and **3**, the *Z*-isomers display improved transport activity relative to the *E*-isomers (Fig. 3B), implying that for these longer derivatives the contracted *Z*-isomer is of sufficient length to reach the relay transporter in the opposite leaflet to exchange the ion and mediate relay transport. The enhanced activity for *Z* over *E* for **2** and **3** suggests that the dissociation of the 2 : 1 transmembrane complex is more facile for the *Z*-configuration, highlighting the role of molecular shape as well as length of the carrier arm in determining the rate of relay ion transport. Azobenzene-containing photo-lipids have previously been shown to modulate the order and dynamics of lipid bilayers,[42,43] and so we tentatively speculate that the *Z*-isomers promote faster transport kinetics by decreasing local order.

The $k_{ini}(Z) > k_{ini}(E)$ activity relationship in the longer derivative **3**, which is reversed, $k_{ini}(E) > k_{ini}(Z)$, for the shorter relay **1**, provides a novel means with which to control relay activity with light: varying the relay arm length switches between the *E* and *Z* isomers being more active, and hence the wavelength with which transport is enhanced. For **1**, off–on activation ($Z \rightarrow E$) is achieved with blue light, and reversed with green, whereas for **3**, off–on activation ($E \rightarrow Z$) is achieved with green light, and reversed with blue.

In conclusion, we have explored the transport activity of a homologous series of photo-switchable relay transporters, revealing that increasing the carrier arm length enhances transport kinetics. Notably, for the longer derivatives **2** and **3** the contracted *Z*-isomer displays increased transport activity relative to the extended *E*-isomer, whilst the reverse is true for the shorter derivative **1**. This provides a mechanism by which to vary the off–on switching direction and excitation wavelength.

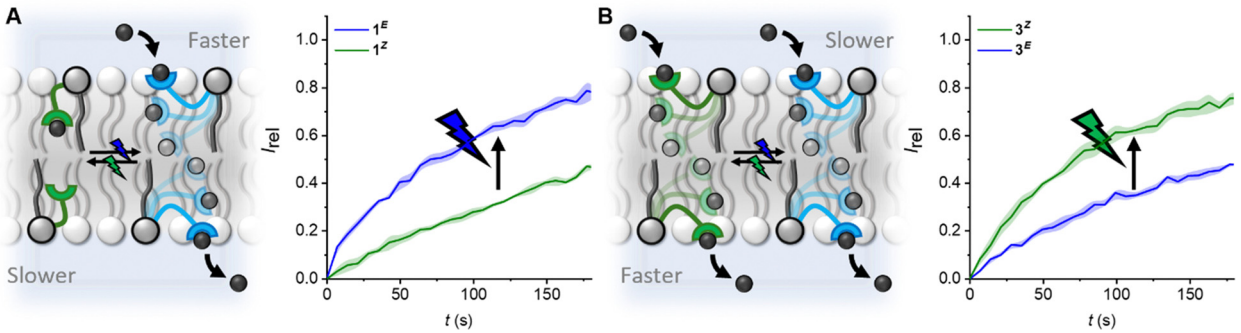

Fig. 3 Modulating the direction and wavelength of off–on switching by tuning the length of the photo-switchable relay transporters. (A) Off(*Z*)-on(*E*) switching facilitated by blue light, and reversed with green light for compound **1**. (B) Off(*E*)–on(*Z*) switching facilitated by green light, and reversed with blue light for compound **3**. Data shown at 5 mol% for **1** and 0.25 mol% for **3**, conditions as in Fig. 2. Data for **1** from ref. 31.

Relay transporters provide a means of probing supramolecular interactions within the complex lipid bilayer environment.

T. G. J. and A. S.-K. synthesised the compounds and conducted the ion transport assays. M. J. L. conceived and supervised the project. T. G. J. wrote the first draft of the manuscript. All authors contributed to data analysis and reviewing and editing of the manuscript.

T. G. J. and M. J. L. thank the Royal Society for funding. T. G. J. thanks Exeter College Oxford for a scholarship. M. J. L. is a Royal Society University Research Fellow.

Data availability

The data supporting this article have been included as part of the ESI.†

Conflicts of interest

There are no conflicts to declare.

Notes and references

‡ For 1,2-dimyristoleoyl-*sn*-glycero-3-phosphocholine (14 : 0 PC) vesicles cholesterol was incorporated at a loading of 7 : 3 lipid to cholesterol to give a fluid membrane at room temperature.

1 P. Läuger, *Angew. Chem., Int. Ed. Engl.*, 1985, **24**, 905–923.
2 A. Barba-Bon, M. Nilam and A. Hennig, *ChemBioChem*, 2020, **21**, 886–910.
3 L. E. Bickerton, T. G. Johnson, A. Kerckhoffs and M. J. Langton, *Chem. Sci.*, 2021, **12**, 11252–11274.
4 A. Mondal, M. Ahmad, D. Mondal and P. Talukdar, *Chem. Commun.*, 2023, **59**, 1917–1938.
5 P. A. Gale, R. Pérez-Tomás and R. Quesada, *Acc. Chem. Res.*, 2013, **46**, 2801–2813.
6 G. Picci, S. Marchesan and C. Caltagirone, *Biomedicines*, 2022, **10**, 885.
7 J. T. Davis, P. A. Gale and R. Quesada, *Chem. Soc. Rev.*, 2020, **49**, 6056–6086.
8 M. J. Langton, *Nat. Rev. Chem.*, 2021, **5**, 46–61.
9 M. Ahmad, S. A. Gartland and M. J. Langton, *Angew. Chem., Int. Ed.*, 2023, **62**, e202308842.
10 J. de Jong, J. E. Bos and S. J. Wezenberg, *Chem. Rev.*, 2023, **123**, 8530–8574.
11 A. Docker, T. G. Johnson, H. Kuhn, Z. Zhang and M. J. Langton, *J. Am. Chem. Soc.*, 2023, **145**, 2661–2668.
12 M. Fares, X. Wu, D. Ramesh, W. Lewis, P. A. Keller, E. N. W. Howe, R. Pérez-Tomás and P. A. Gale, *Angew. Chem., Int. Ed.*, 2020, **59**, 17614–17621.
13 R. B. P. Elmes, N. Busschaert, D. D. Czech, P. A. Gale and K. A. Jolliffe, *Chem. Commun.*, 2015, **51**, 10107–10110.
14 E. N. W. Howe, N. Busschaert, X. Wu, S. N. Berry, J. Ho, M. E. Light, D. D. Czech, H. A. Klein, J. A. Kitchen and P. A. Gale, *J. Am. Chem. Soc.*, 2016, **138**, 8301–8308.
15 X. Wu, J. R. Small, A. Cataldo, A. M. Withecombe, P. Turner and P. A. Gale, *Angew. Chem., Int. Ed.*, 2019, **58**, 15142–15147.
16 Y. R. Choi, B. Lee, J. Park, W. Namkung and K. S. Jeong, *J. Am. Chem. Soc.*, 2016, **138**, 15319–15322.
17 M. Ahmad, T. G. Johnson, M. Flerin, F. Duarte and M. J. Langton, *Angew. Chem., Int. Ed.*, 2024, **63**, e202403314.
18 S. J. Wezenberg, L. J. Chen, J. E. Bos, B. L. Feringa, E. N. W. Howe, X. Wu, M. A. Siegler and P. A. Gale, *J. Am. Chem. Soc.*, 2022, **144**, 331–338.
19 D. Villarón, J. E. Bos, F. Kohl, S. Mommer, J. de Jong and S. J. Wezenberg, *J. Org. Chem.*, 2023, **88**, 11328–11334.
20 A. Kerckhoffs and M. J. Langton, *Chem. Sci.*, 2020, **11**, 6325–6331.
21 Y. R. Choi, G. C. Kim, H. G. Jeon, J. Park, W. Namkung and K. S. Jeong, *Chem. Commun.*, 2014, **50**, 15305–15308.
22 S. B. Salunke, J. A. Malla and P. Talukdar, *Angew. Chem., Int. Ed.*, 2019, **58**, 5354–5358.
23 M. Ahmad, S. Metya, A. Das and P. Talukdar, *Chem. – Eur. J.*, 2020, **26**, 8703–8708.
24 S. A. Gartland, T. G. Johnson, E. Walkley and M. J. Langton, *Angew. Chem., Int. Ed.*, 2023, **62**, e202309080.
25 X. Chao, T. G. Johnson, M. C. Temian, A. Docker, A. L. D. Wallabregue, A. Scott, S. J. Conway and M. J. Langton, *J. Am. Chem. Soc.*, 2024, **146**, 4351–4356.
26 J. N. Martins, B. Raimundo, A. Rioboo, Y. Folgar-Cameán, J. Montenegro and N. Basílio, *J. Am. Chem. Soc.*, 2023, **145**, 13126–13133.
27 T. G. Johnson and M. J. Langton, *J. Am. Chem. Soc.*, 2023, **145**, 27167–27184.
28 J. Shen, C. Ren and H. Zeng, *Acc. Chem. Res.*, 2022, **55**, 1148–1159.
29 B. A. McNally, E. J. O'Neil, A. Nguyen and B. D. Smith, *J. Am. Chem. Soc.*, 2008, **130**, 17274–17275.
30 T. G. Johnson, A. Docker, A. Sadeghi-Kelishadi and M. J. Langton, *Chem. Sci.*, 2023, **14**, 5006–5013.
31 T. G. Johnson, A. Sadeghi-Kelishadi and M. J. Langton, *J. Am. Chem. Soc.*, 2022, **144**, 10455–10461.
32 R. Ye, C. Ren, J. Shen, N. Li, F. Chen, A. Roy and H. Zeng, *J. Am. Chem. Soc.*, 2019, **141**, 9788–9792.
33 C. Ren, F. Chen, R. Ye, Y. S. Ong, H. Lu, S. S. Lee, J. Y. Ying and H. Zeng, *Angew. Chem., Int. Ed.*, 2019, **58**, 8034–8038.
34 S. Chen, Y. Wang, T. Nie, C. Bao, C. Wang, T. Xu, Q. Lin, D. H. Qu, X. Gong, Y. Yang, L. Zhu and H. Tian, *J. Am. Chem. Soc.*, 2018, **140**, 17992–17998.
35 C. Wang, S. Wang, H. Yang, Y. Xiang, X. Wang, C. Bao, L. Zhu, H. Tian and D. H. Qu, *Angew. Chem., Int. Ed.*, 2021, **60**, 14836–14840.
36 D. Bléger, J. Schwarz, A. M. Brouwer and S. Hecht, *J. Am. Chem. Soc.*, 2012, **134**, 20597–20600.
37 C. Knie, M. Utecht, F. Zhao, H. Kulla, S. Kovalenko, A. M. Brouwer, P. Saalfrank, S. Hecht and D. Bléger, *Chem. – Eur. J.*, 2014, **20**, 16492–16501.
38 W. Huang and D. G. Levitt, *Biophys. J.*, 1977, **17**, 111–128.
39 G. Gramse, A. Dols-Perez, M. A. Edwards, L. Fumagalli and G. Gomila, *Biophys. J.*, 2013, **104**, 1257–1262.
40 Y. Liu, A. Sengupta, K. Raghavachari and A. H. Flood, *Chem*, 2017, **3**, 411–427.
41 X. Wu, P. Wang, W. Lewis, Y. B. Jiang and P. A. Gale, *Nat. Commun.*, 2022, **13**, 1–7.
42 M. Doroudgar, J. Morstein, J. Becker-Baldus, D. Trauner and C. Glaubitz, *J. Am. Chem. Soc.*, 2021, **143**, 9515–9528.
43 P. Urban, S. D. Pritzl, M. F. Ober, C. F. Dirscherl, C. Pernpeintner, D. B. Konrad, J. A. Frank, D. Trauner, B. Nickel and T. Lohmueller, *Langmuir*, 2020, **36**, 2629–2634.